Chromatofocusing Fails To Separate hFSH Isoforms on the Basis of Glycan Structure†

George R. Bousfield,*,‡ Vladimir Y. Butnev,‡ Jean-Michel Bidart,§ Dilusha Dalpathado,|| Janet Irungu,|| and Heather Desaire||

Department of Biological Sciences, Wichita State University, Wichita, Kansas 67260, Departement Biologie Clinique, Institut Gustave-Roussy, Villejuif, France, and Chemistry Department, University of Kansas, Lawrence, Kansas 66045

Received August 29, 2007; Revised Manuscript Received November 7, 2007

ABSTRACT: Follicle-stimulating hormone (FSH) glycosylation is regulated by feedback from the gonads, resulting in an array of glycans associated with FSH preparations derived from pools of pituitary or urine extracts. FSH glycosylation varies due to inhibition of FSHβ N-glycosylation, elaboration of 1−4 branches possessed by mature N-glycans, and the number and linkage of terminal sialic acid residues. To characterize FSH glycosylation, FSH isoforms in pituitary gland extracts and a variety of physiological fluids are commonly separated by chromatofocusing. Variations in the ratios of immunological and biological activities in the resulting FSH isoform preparations are generally attributed to changes in glycosylation, which are most often defined in terms of sialic acid content. Using Western blotting to assess human FSHβ glycosylation inhibition revealed 30−47% nonglycosylated hFSHβ associated with four of six hFSH isoform preparations derived by chromatofocusing. Glycopeptide mass spectrometry assessment of glycan branching in these isoforms extensively characterized two N-glycosylation sites, one at αAsn^{52}, the critical glycan for FSH function, and the other at βAsn^{24}. With two to four N-glycans per FSH molecule, many combinations of charges distributed over these sites can provide the same isoelectric point. Indeed, several glycans were common to all isoform fractions that were analyzed. There was no trend showing predominantly monoantennary glycans associated with the high-pI fractions, nor were predominantly tri- and tetra-antennary glycans associated with low-pI fractions. Thus, differences in receptor binding activity could not be associated with any specific glycan type or location in the hormone. FSH aggregation was associated with reduced receptor binding activity but did not affect immunological activity. However, as gel filtration indicated sufficient heterodimer was present in each isoform preparation to generate complete inhibition curves, the near total loss of receptor binding activity in several preparations could not be explained by aggregation alone, and the mechanism remains unknown.

The pituitary glycoprotein hormones are unusual members of the cystine-knot growth factor superfamily (*1*, *2*). The former are not synthesized as prohormones and require N-glycosylation for full expression of biological activity. Moreover, both α and β subunits are glycosylated. As various aspects of glycosylation appear to be under physiological regulation and because most glycoprotein hormones are derived from thousands of individuals in a variety of physiological conditions, a bewildering array of glycans can be associated with glycoprotein hormone preparations. For example, as many as 105 glycan structures have been identified in oligosaccharide preparations obtained from a single eLH[1] N-glycosylation site by a combination of high-pH anion exchange chromatography and mass spectrometry (*3*). At the other extreme, hCG appeared to possesses only two to four glycans per site on the basis of NMR studies (*4*). Mass spectrometry procedures confirmed two glycans at hCGβ Asn^{30}, but seven glycans appeared to be attached at Asn^{13} (*5*). A more recent hCGβ glycopeptide mass spectrometry study identified 14 glycans at Asn^{13} and 11 at Asn^{30} (*6*). Using a variety of separation techniques, including anion exchange chromatography, zone electrophoresis, isoelectric focusing, and chromatofocusing, glycoprotein hormone preparations can be separated into several isoform fractions (*7*). Highly sensitive radioimmunoassays have permitted detection of changes in isoform patterns under differing physiological conditions that have been attributed to changes in glycosylation. Isoform patterns for pituitary, serum, and urinary FSH were strikingly different, suggesting

† This project was supported by NIH Grants P20 RR16475 from the INBRE Program and P20 RR017708 from the COBRE Program of the National Center for Research Resources, National Science Foundation Grant EPS-9874732, and matching support from the State of Kansas.

* To whom correspondence should be addressed: Department of Biological Sciences, Wichita State University, 1845 Fairmount, Wichita, KS 67260. Phone: (316) 987-6088. Fax: (316) 978-3772. E-mail: george.bousfield@wichita.edu.

‡ Wichita State University.

§ Institut Gustave-Roussy.

|| University of Kansas.

[1] Abbreviations: FSH, follicle-stimulating hormone [lowercase letter preceding FSH indicates the species of origin: h, human; e, equine (horse); o, ovine (sheep)]; LH, luteinizing hormone; TSH, thyroid-stimulating hormone; HPLC, high-performance liquid chromatography; RIA, radioimmunoassay; RLA, radioligand receptor assay; M_r, relative molecular weight; =PhNCS, phenylthiohydantoin derivative.

10.1021/bi701764w CCC: $40.75
Published on Web 01/16/2008

differential FSH secretion by the pituitary and extensive FSH metabolism in the kidney or selective retention of FSH isoforms by other organs, such as the liver (*7*). The same procedure applied to postmenopausal urinary gonadotropin pharmaceutical preparations of varying purity also resulted in striking alterations in FSH isoform populations. This suggested that the isoform patterns were influenced by the presence or absence of other proteins.

Because most gonadotropin isoform separations are typically performed on crude tissue extracts and unpurified physiological fluids, the glycosylation patterns supposedly responsible for isoform separation are unknown. A series of studies that measured sialic acid content in hFSH isoform preparations obtained by preparative isoelectric focusing suggested that FSH glycan branching was primarily responsible for decreasing isoform isoelectric points (*8*−*10*). A study in our laboratory involving hFSH fractionated by the more commonly employed isoform isolation method, chromatofocusing, revealed the presence of two major hFSH glycoforms that could be distinguished on the basis of all-or-none FSHβ glycosylation (*11*). The hFSH glycoform lacking β subunit glycans (hereafter designated diglycosylated hFSH because it is only glycosylated on the α subunit) was present in all isoform fractions, including the most acidic. Therefore, glycan branching alone could not account for the reduction in the apparent pI because 13 sialic acid-terminated branches distributed between only two glycans exceeded the theoretical limit of five branches for N-glycans in general and the experimentally determined limit of four branches per oligosaccharide based on known hFSH glycan structures (*12*−*15*).

Because the most interesting hFSH glycoform preparations encountered in our earlier study were limited in abundance, we have been developing methods for efficiently characterizing gonadotropin N-glycosylation (*15*−*17*). Recently, we reported that mass spectrometry analysis of FSH glycopeptides could provide simultaneous, site-specific analysis of multiple N-glycosylation sites (*15*). In this study, we applied these and other techniques to the analysis of hFSH isoforms prepared by chromatofocusing. As these isoforms exhibited the same level of immunological activity yet differed significantly in their receptor binding activity, they represented classical FSH isoform preparations. However, examination of glycosylation at αAsn^{52} and βAsn^{24} revealed that chromatofocusing had not even enriched the acidic isoforms for highly branched glycans. In fact, the glycopeptide mixtures isolated from five isoform preparations that were analyzed possessed many of the same glycans.

EXPERIMENTAL PROCEDURES

Materials. A 107 mg sample of hFSH preparation AFP-4161B was obtained from the National Pituitary Hormone Program and A. F. Parlow by D. N. Ward (retired, M. D. Anderson Cancer Center, Houston, TX). The reported FSH biological potency of this preparation is 4941 IU/mg (*18*). Comparison with the current National Hormone and Pituitary Program hFSH preparation (8560 IU/mg) in a recent FSH steroidogenesis assay yielded a 7120 IU/mg potency estimate for AFP-4161B, suggesting no loss of biological activity in storage. AFP-4161B subjected to chromatofocusing produced the hFSH isoform preparations used in this study. All hFSH preparations were stored in polyethylene vials as lyophilized powders. Samples used in analytical studies below were removed from the vials and weighed on a Cahn (ThermoScientific, Waltham, MA) model C-31 microbalance. Dry weight was the basis of comparison throughout this study because the presence of a 39 500 M_r contaminant (*19*) reduced the purity of all hFSH preparations below 95%, which is required for accurate FSH protein determination by single-hydrolysis amino acid analysis.

FSH Chromatofocusing. Chromatofocusing resins and buffers were obtained from GE Healthcare (Piscataway, NJ). A 96.3 mg sample of purified hFSH (AFP-4161B) was dissolved in 4 mL of 0.025 M imidazole-HCl (pH 7.4). The sample was applied to a 1 cm × 26 cm PBE94 column that had been previously equilibrated with 400 mL of the same buffer. The pH gradient was developed with Polybuffer 74, which had been adjusted to a pH of 4.0 with HCl at a flow rate of 12.5 mL/h. Twelve-minute fractions were collected, each of which contained 2.5 mL of column effluent. The pH for each fraction was measured with a pH meter and the absorbance measured at 280 nm using a spectrophotometer. Protein still bound to the column at pH 4 was removed by elution with 1 M NaCl. Pooled fractions were lyophilized and ampholines removed by gel filtration over a 2.5 cm × 85 cm Sephadex G-75 column equilibrated and developed with 0.126 M ammonium bicarbonate buffer. FSH isoforms were recovered by lyophilization.

FSH RIA. FSH radioimmunoassays were performed using hFSH heterodimeric-specific monoclonal FSH25 or hFSHβ subunit-specific monoclonal antibody RFSH20 and [^{125}I]-hFSH tracer using a previously described protocol (*20*). The antibodies were diluted 1:1000 with 0.05 M sodium phosphate buffer (pH 7.5) containing 0.5% BSA and 0.05% sodium azide (RIA buffer). Samples of hFSH preparation AFP-4161B or hFSH isoform samples were weighed and serially diluted with RIA buffer. Aliquots of each dilution placed in duplicate 12 mm × 75 mm polypropylene tubes containing antibody and 30000 cpm [^{125}I]hFSH were incubated overnight at 4 °C. Separation of bound and unbound hFSH was initiated by addition of 100 μL of RIA buffer-diluted calf serum (1:3 serum:RIA buffer) and 1 mL of a 20% polyethylene glycol 6000 solution to precipitate the antibody−hormone complexes. This was followed by centrifugation at 4000 rpm for 40 min and aspiration of the unbound hormone in the supernatant. The pellets were counted in a Packard (Downers Grove, IL) Cobra II gamma counter. Statistical analysis of dose−response curves was conducted using GraphPad Software, Inc. (San Diego, CA), Prism, version 4, for Macintosh.

FSH RLA. The Wichita State University institutional animal care and use committee approved all procedures involving animals. Receptor binding assays were performed using 25 mg of rat testis homogenate tissue or 250000 hFSH receptor-expressing CHO cells/tube and 2.5 ng of [^{125}I]eFSH (*21*). FSH samples were weighed, dissolved in RLA buffer, and serially diluted with additional RLA buffer. Duplicate assay tubes containing hFSH samples, tracer, and receptor preparation were incubated for 2 h at 37 °C in a shaking water bath and then centrifuged at 4000 rpm for 30 min, and the supernatant was aspirated and the pellet counted in a Packard Cobra II gamma counter. Statistical analysis of dose−response curves was conducted using Prism.

SDS−PAGE. Samples containing 5−20 μg of purified hFSH or 5 μg of chromatofocusing fraction lyophilized protein were subjected to SDS−PAGE on a 15% polyacrylamide mini slab gel under reducing conditions (*11*). Electrophoresis was carried out at 200 V, a constant voltage in a Bio-Rad (Hercules, CA) Protean III mini-gel apparatus. The gel was Coomassie stained with GelCode Blue (Pierce Chemical Co., Rockford, IL).

Western Blotting. Samples containing 0.5−2 μg of purified hFSH or 1 μg of chromatofocusing fractions were subjected to SDS−PAGE on 15% polyacrylamide mini-gels under reducing conditions (*11*). Each gel was electrotransferred to an Immobilon-P PVDF membrane (GE Healthcare), which was subsequently blocked with 5% nonfat dry milk in Western blotting buffer overnight. The following morning, each membrane was incubated with either anti-FSHβ monoclonal antibody RFSH20 or anti-α subunit monoclonal antibody HT13. After being incubated and washed, both membranes were incubated with the rabbit anti-mouse IgG−HRP complex. After being incubated and washed, each membrane was incubated with Amersham ECL Plus (GE Healthcare) chemiluminescence reagent. The FSH bands were detected using a Bio-Rad VersaDoc 4000 instrument. Band intensities were determined using the Bio-Rad software package Quantity One.

Glycopeptide Isolation. Glycopeptides were derived from hFSH samples by proteinase K digestion followed by Superdex peptide column gel filtration (*15*). The hFSH isoform samples were dissolved in 0.1 M sodium phosphate buffer containing 6 M guanidine-HCl and 10 mM EDTA, reduced by the addition of 20 mM DTT, and carboxymethylated by addition of 100 mM iodoacetic acid following our usual procedures (*22*). The reduced, alkylated hFSH preparations were desalted using Amicon Ultra-4 centrifugal ultrafiltration cartridges, and the reaction buffer was replaced with 0.2 M ammonium bicarbonate (pH 8.5). The denatured hFSH preparations were incubated with proteinase K (1:10, w/w) at 37 °C overnight and then dried by evaporation in a Thermo Savant (Waltham, MA) Speed Vac. The digest was resuspended in 175 μL of 0.2 M ammonium bicarbonate and the glycopeptide fraction isolated by gel filtration over a GE Healthcare Superdex peptide column. The HPLC system consisted of a Waters (Milford, MA) model 600 quaternary solvent delivery system and model 484 tunable absorbance monitor, which were controlled by the Waters Empower software system running on a Dell (Roundtop, TX) Dimension model 8250 computer. The Superdex peptide column was equilibrated with 0.2 M ammonium bicarbonate and the chromatogram developed with the same buffer at a flow rate of 0.4 mL/min. Fractions were collected by hand and peptides and glycopeptides recovered by evaporation.

Mass Spectrometry. MS data were acquired on a high-resolution Thermo Finnigan (San Jose, CA) linear ion trap-Fourier transform ion cyclotron resonance mass spectrometer (LTQ-FTICR-MS) equipped with a 7 T actively shielded magnet (*15*). The dried glycopeptides were first dissolved in water and diluted with a MeOH/H_2O mixture (4:1) containing 0.3% acetic acid, to a final concentration of 0.03 μg/μL. Samples were directly infused into the mass spectrometer using a syringe pump at a flow rate of 5 μL/min. High-resolution data were acquired by maintaining the resolution at 50000, for *m*/*z* 400. The instrument was externally calibrated over the mass range of interest (*m*/*z* 800−2000) prior to the analysis. ESI spray voltage was maintained between −3.0 and −4.0 kV for data acquisition in the negative mode. The capillary temperature was held between 200 and 230 °C, and N_2 was used as a nebulizing gas at 20 psi. Data were acquired and processed using Xcalibur, version 1.4 SR1 (Thermo Finnigan).

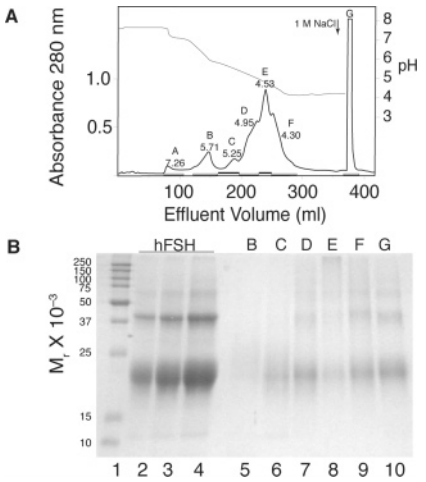

FIGURE 1: Isoforms derived from hFSH by chromatofocusing. (A) Chromatogram showing elution of hFSH isoforms from pooled pituitary hFSH (AFP-4161B). The dotted line shows the pH gradient that developed the chromatogram. Proteins still retained at pH 4 were eluted with 1 M NaCl (arrow). (B) SDS−PAGE analysis of isoform fractions under reducing conditions followed by Coomassie Blue staining. Protein amounts are dry weights determined with a Cahn microbalance: lane 1, Bio-Rad Precision MW markers as indicated; lanes 2−4, 5, 10, and 20 μg of hFSH (AFP-4161B), respectively; lane 5, 5 μg of hFSH-B; lane 6, 5 μg of hFSH-C; lane 7, 5 μg of hFSH-D; lane 8, 5 μg of hFSH-E; lane 9, 5 μg of hFSH-F; and lane 10, 5 μg of hFSH-G.

RESULTS

hFSH Isoform Preparation. The purified hFSH preparation AFP-4161B was separated into seven fractions, designated hFSH-A−hFSH-G, by chromatofocusing using a pH 7 to 4 gradient (Figure 1A). FSH isoform preparations were recovered from all fractions, except fraction A, which did not contain detectable protein following Sephadex G-75 chromatography (Table 1). The total weight recovery was 90 mg (93%). SDS−PAGE followed by Coomassie blue staining revealed hFSH subunits to be the most abundant component in each isoform preparation (Figure 1B). Densitometric analysis of the hFSH subunit region of the gel (the α subunit band partially overlaps the 21000 and 24000 M_r hFSHβ bands) indicated each 5 μg isoform sample included an average of 2.1 μg of FSH (Table 2) on the basis of a comparison of isoform FSH subunit band density with that of 5 μg of hFSH AFP-4161B (Figure 1B, lane 2). This indicated only 43% total hFSH recovery, which was lower than the weight and immunological activity recovery esti-

Table 1: FSH Isoform Recovery from 96.3 mg of AFP-4161B Based on Mass, Immunoreactivity, and Receptor Binding Activity

preparation	FSH recovery (mg)[a]	FSH recovery by densitometry milligram equivalent[b]	FSH heterodimer immunoreactivity milligram equivalent[c]	FSHβ subunit immunoreactivity milligram equivalent[d]	hFSHR activity recovered milligram equivalent[e]	rFSHR activity recovered milligram equivalent[f]
hFSH-B	3.6	0.9	0.6	0.6	1.0	0.04
hFSH-C	5.1	2.1	3.0	3.7	3.8	2.4
hFSH-D	17.1	8.9	16.0	14.9	–	–
hFSH-E	16.2	4.2	13.1	9.6	–	–
hFSH-F	17.9	9.0	15.5	9.1	–	–
hSFH-G	30.1	18.1	35.5	24.4	–	–
total recovery (mg)	90.0	43.2	83.7	62.3	4.8	2.44
% recovery[g]	93	45	87	65	5	3

[a] Dry weight recovery of lyophilized protein powder after ampholine removal. Fraction A is not included because no protein was recovered. [b] Determined by relative densitometry of Coomassie-stained FSH subunit bands for 5 μg (dry weight) samples following SDS−PAGE (Figure 1B) and weight recovery (Table 1). [c] Determined from hFSH heterodimer immunoactivity (Figure 2A) and weight recovery (Table 1). [d] Determined from hFSHβ subunit immunoactivity (Figure 2B) and weight recovery (Table 1). [e] Determined from hFSHR binding activity (Figure 3A) and weight recovery (Table 1). [f] Determined from rFSHR binding activity (Figure 3B) and weight recovery (Table 1). [g] Relative to 96.3 mg of hFSH AFP-4161B fractionated by chromatofocusing.

Table 2: FSH Isoform Characteristics

preparation	pI	FSH (μg)[a]	HT13, % subunit[b]	RFSH20, % subunit[c]	% 21 kDa hFSHβ[d]	% dimer (HPLC)[e]
AFP-4161B	N/A[f]	5	85	95	33	72
hFSH-B	5.71	1.2	94	77	39	100
hFSH-C	5.25	2.1	89	75	37	86
hFSH-D	4.95	2.6	51	70	47	40
hFSH-E	4.53	1.3	37	44	N/A[f]	25
hFSH-F	4.30	2.5	40	74	47	42
hFSH-G	<4.0	3.0	53	79	30	43

[a] Determined by densitometry of Coomassie-stained bands following SDS−PAGE (Figure 1B). [b] Relative density of the α subunit band following α-specific (HT13) Western blot (Figure 4B). [c] Relative density of the β subunit band following FSHβ-specific (RFSH20) Western blot (Figure 4A). [d] Relative abundance of the 21 kDa hFSHβ band, representing diglycosylated hFSH (*23*). [e] Relative area under the heterodimer peak as compared with aggregated hFSH and subunit peak areas (Figure 8). [f] Not applicable.

mates (Table 1). Subunit staining was very weak for hFSH-B and less intense for hFSH-E, which averaged 1.3 μg equivalent of FSH subunit density. The latter possessed a high-MW aggregate that barely entered the top of the gel (lane 8). High-M_r bands contributed to the low apparent protein recovery based on subunit band density. The 39 500 M_r unidentified protein contaminant of hFSH AFP-4161B (lanes 2−4) was present as a more diffuse band in isoform fractions hFSH-D−hFSH-G (lanes 6−9). This was confirmed by subunit dissociation and gel filtration performed on aliquots of these preparations (unpublished data).

The hFSH content of each isoform fraction was measured by a heterodimer-specific RIA using the FSH dimer-specific monoclonal antibody FSH25 (Figure 2A). FSH heterodimer immunological activity recoveries totaled 87% (Table 1). Isoform preparation hFSH-B was significantly lower in FSH content than AFP-4161B ($P < 0.0001$) and all other hFSH isoform preparations [$P < 0.0001$ (Table 3)]. This was subsequently found to be due to incomplete ampholine removal. Residual ampholine was also associated to a lesser extent with eFSH-C (see panels A and B of Figure 8). The activities of all other isoform preparations were similar, although the differences were statistically significant for all but hFSH-D and hFSH-G ($P = 0.1534$).

An FSHβ-specific monoclonal antibody RFSH20 RIA (Figure 2B) indicated a similar pattern of hFSH abundance for isoforms C−G, with much lower immunological activity

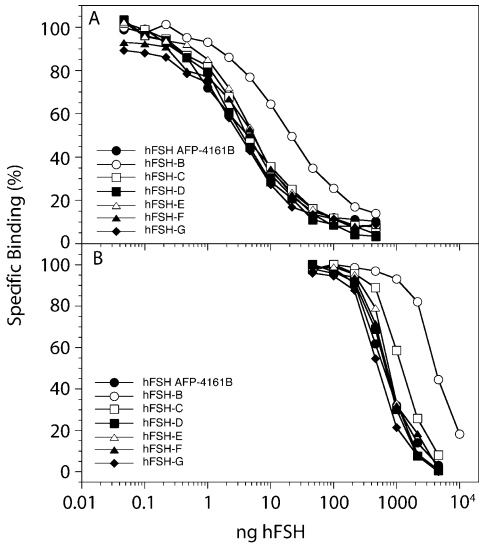

FIGURE 2: Quantitation of hFSH in isoform preparations by a radioimmunoassay. The [^{125}I]hFSH tracer was displaced by increasing amounts of hFSH or isoform preparations (dry weight), as indicated. (A) FSH immunoactivity detected by heterodimer-specific monoclonal antibody FSH25. (B) FSHβ immunoactivity detected by FSHβ-specific monoclonal antibody RFSH20.

Table 3: FSH Immunoactivity Associated with Each hFSH Isoform Preparation

FSH preparation	MAb RFSH20 ID_{50} (ng) (95% confidence limit)	MAb RFSH20 relative potency (IU/mg)	MAb FSH25 ID_{50} (ng) (95% confidence limit)	MAb FSH25 relative potency (IU/mg)
AFP-4161B	626 (592−662)	4941	2.7 (2.29−3.09)	4941
hFSH-B	3432 (3203−3677)[a]	889	16.5 (12.5−21.8)[a]	791
hFSH-C	1076 (1017−1139)[a]	2866	3.7 (3.2−4.3)[a]	3558
hFSH-D	665 (647−683)[a]	4644	3.1 (2.7−3.5)[a]	4299
hFSH-E	769 (752−787)[a]	4002	4.5 (4.0−5.1)[a]	2915
hFSH-F	719 (643−803)[a]	4299	5.2 (4.5−6.1)[a]	2520
hFSH-G	528 (505−553)[a]	5830	3.3 (2.9−3.7)[a]	4002

[a] Significantly different from that of hFSH (AFP-4161B); $P = 0.0427$ to <0.0001.

for hFSH-B (Table 3). Total FSHβ immunoactivity recovery was only 65% with this antibody (Table 1). Although hFSH-D and hFSH-G immunoactivities were close to or greater than that of AFP-4161B, the differences remained significant ($P = 0.0427$ and $P < 0.0001$, respectively). However, considerably higher FSH concentrations were

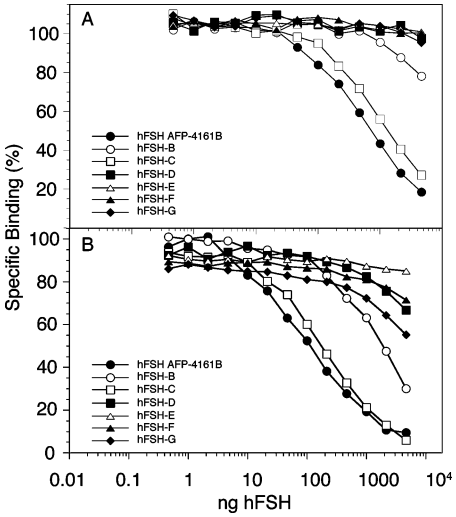

FIGURE 3: FSH receptor binding assay. (A) FSH receptor binding assay using [^{125}I]eFSH tracer and CHO cells expressing human FSHR. (B) FSH receptor binding assay using [^{125}I]eFSH tracer and rat testis homogenate receptor preparation. The curve for hFSH-B appears nonparallel, although the extent of inhibition permitted determination of ID_{50} (Table 4). The hormone preparations and the masses of lyophilized powder used to displace the tracer are given.

Table 4: FSH Receptor Binding Activity Associated with hFSH Isoform Preparations

	human FSH receptors		rat FSH receptors	
FSH preparation	ID_{50} (ng) (95% confidence limit)	relative potency (IU/mg)	ID_{50} (ng) (95% confidence limit)	relative potency (IU/mg)
AFP-4161B	330 (290−376)	4941	92 (75−114)	4941
hFSH-B	1205 (905−1606)[a]	1334	8201 (821−81900)[a,b]	49
hFSH-C	446 (362−549)[a]	3656	197 (157−248)[a]	2322
hFSH-D				
hFSH-E				
hFSH-F				
hFSH-G				

[a] Signifcantly different from that of hFSH (AFP-4161B); $P = 0.0325$ to <0.0001. [b] The inhibition curve appears to be nonparallel to AFP-4161B (Figure 3B).

necessary to displace the [^{125}I]hFSH tracer from this antibody than from the dimer-specific antibody.

The FSH receptor binding activity of each isoform preparation was measured in a human FSH receptor binding assay (Figure 3A). Only isoform preparation hFSH-C displaced more than 50% of the [^{125}I]eFSH, thereby exhibiting quantifiable FSH receptor binding activity of 3656 IU/mg relative to AFP-4161B (Table 4), but increasing to 5078 IU/mg, 103% of that of AFP-4161B, when normalized for FSH immunoactivity using dimer-specific antibody FSH25 (Table 3). Comparison of the isoform preparations in a rat testis FSH receptor binding assay (Figure 3B) indicated that hFSH-C was significantly more active than any other isoform preparation (Table 4). Its potency was 2322 IU/mg, 79% as active as AFP-4161B. Isoform preparation hFSH-B had a value of only 49 IU/mg, 1% as active as AFP-4161B. When the weight-based ID_{50} was recalculated on the basis of hFSH-B activity in the heterodimer RIA, it was still only 346 IU/mg, 7% as active as AFP-4161B. The relative receptor binding activities for the remaining preparations, which for the most part only partially inhibited [^{125}I]eFSH binding, were ordered as follows: hFSH-G > hFSH-D = hFSH-F > hFSH-E. The last of these had no detectable FSH receptor binding activity up to a concentration of 9.28 μg/mL. Receptor binding assays indicated only 3−5% recovery of FSH activity (Table 1).

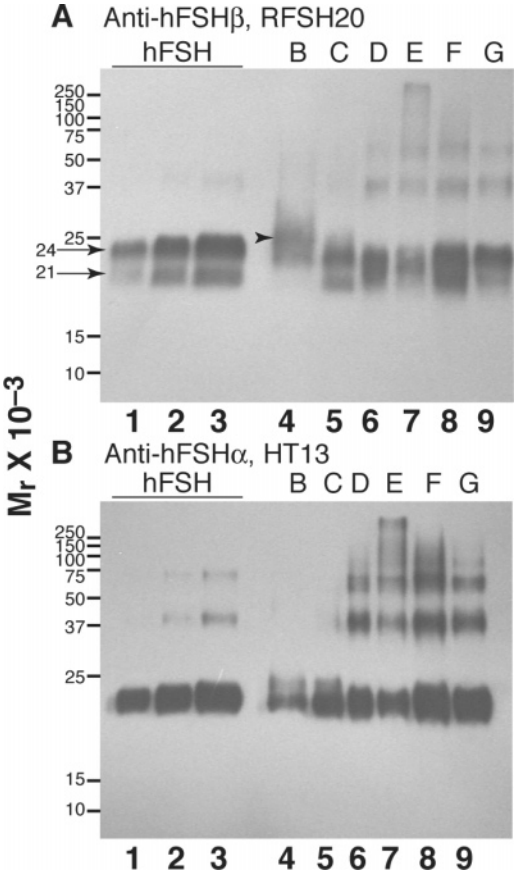

FIGURE 4: FSH subunit Western blot. (A) FSHβ Western blot of reduced samples of chromatofocusing fractions B−G, as indicated. The primary antibody was anti-hFSHβ monoclonal antibody RFSH20. (B) FSHα Western blot of the same samples shown in panel A. Note that hFSH-C has no aggregated forms while hFSH-E has the most extensive range of aggregated FSH. The primary antibody was anti-hCGα monoclonal antibody HT13. Immunoreactive subunit bands were detected by chemiluminescence. Positions of the Bio-Rad Precision prestained MW markers are indicated. Arrows indicate the 24000 and 21000 M_r bands that represent glycosylated and nonglycosylated hFSHβ, respectively. The arrowhead indicates the 25000 M_r hFSHβ band associated with hFSH-B: lanes 1−3, 0.5, 1, and 2 μg of hFSH (AFP-4161B, respectively); lane 4, 1 μg of hFSH-B; lane 5, 1 μg of hFSH-C; lane 6, 1 μg of hFSH-D; lane 7, 1 μg of hFSH-E; lane 8, 1 μg of hFSH-F; and lane 9, 1 μg of hFSH-G.

Diglycosylated and tetraglycosylated hFSH glycoform abundance in hFSH preparations is indicated by relative densities of two FSHβ-immunoactive bands (*11*, *23*). Western blot analysis of all hFSH isoform preparations indicated the presence of both 24000 M_r glycosylated and 21000 M_r nonglycosylated hFSHβ bands in all but fractions B and E (Figure 4A). Fraction E appeared to be almost exclusively tetraglycosylated hFSH. Isoform fraction hFSH-B possessed two hFSHβ bands migrating at M_r values of 25000 and 24000. We did not know if the 25000 M_r band represented a variant of the 24000 M_r diglycosylated band, perhaps possessing larger glycans and thereby exhibiting a retarded mobility. This uncertainty precluded identification by Western blotting alone. Nonglycosylated, 21000 M_r hFSHβ abundance ranged from 30 to 47%, indicating the majority

of the hFSH present in each isoform fraction was tetraglycosylated hFSH (Table 2). Moreover, there was no direct correlation between pI and glycoform abundance, as tetraglycosylated hFSH constituted 63, 53, 53, and 70% of isoform preparations hFSH-C, -D, -F, and -G, respectively. FSH aggregation was indicated by the presence of 35000, 50000, 75000, and 250000 M_r bands present in isoform fractions hFSH-D, -E, -F, and -G, respectively. The proportion of hFSH subunit immunoactivity migrating in the subunit region of the gel ranged from 44 to 95% in hFSH isoform preparations. It also varied depending on whether the α-specific or FSHβ-specific antibodies were used (Table 2), yet most immunoreactive subunit densities were comparable to that of AFP-4161B, unlike those of Coomassie-stained subunits. Aggregation seemed largely restricted to the more acidic isoform preparations, as only in the 2 μg AFP-4161B hFSH samples was the 35000 M_r aggregate band visible (lane 3). The α subunit migrated as a single immunoreactive band in most isoform preparations (Figure 4B). Some variation in FSHα mobility was associated with isoform fractions hFSH-B and hFSH-C; however, there was not enough protein remaining to investigate the basis for the altered electrophoretic mobility. FSH aggregation was more readily apparent in the α subunit blot, as 37−50% of the α immunoreactivity migrated in the subunit region of the gel for the more acidic isoforms. The remaining density was associated with the bands migrating in the 35000−250000 M_r region of the gel. While aggregated hFSH could now be visualized in the 1 μg sample of hFSH, band intensity was much weaker in lanes 1−3 than in those associated with the four most acidic hFSH isoform preparations (lanes 6−9).

Glycopeptide gel filtration chromatograms indicated differences in glycan size that correlated with a lower isoelectric point (Figure 5). Isoform preparation hFSH-C apparently possessed more smaller-sized glycans than larger-sized glycans, hFSH-G more larger-sized glycans than smaller-sized, while hFSH-D, hFSH-E, and hFSH-F roughly equivalent amounts of both large and small glycans.

Peptide identification by automated Edman degradation of each glycopeptide fraction revealed two abundant phenylthiohydantoin (═PhNCS) derivatives, ═PhNCS-Lys and ═PhNCS-Ile, in cycle 1, which corresponded to glycopeptides KN$^{\alpha 52}$VT and IN$^{\beta 24}$TT, respectively (Table 5). The amino acid derivatives, ═PhNCS-His and ═PhNCS-Ile, in cycle 2 indicated the other two glycopeptides, N$^{\alpha 78}$HT and N$^{\beta 7}$IT, respectively. The yields of both cycle 2 residues were lower than the yields associated with the other two glycopeptides identified in cycle 1. This would have made sense if both cycle 1 residues were derived from the glycosylated α subunit and both cycle 2 residues were derived from the mixture of glycosylated and nonglycosylated hFSHβ. However, one peptide was derived from the α subunit while the other from the β subunit. Because the yields of ═PhNCS amino acid derivatives decreased rapidly, we speculated that the low yield of the peptides identified in cycle 2 represented peptide wash-out after separation from the glycosylated Asn residue, as glycosylation is known to keep the ═PhNCS-Asn^{CHO} derivative in the Edman chemistry cartridge. Accordingly, we covalently attached the glycopeptides to Sequelon−arylamine membranes and repeated the Edman degradation experiment. The results listed in Table 6 indicate that the high yield of ═PhNCS-Lys reflects the actual yield

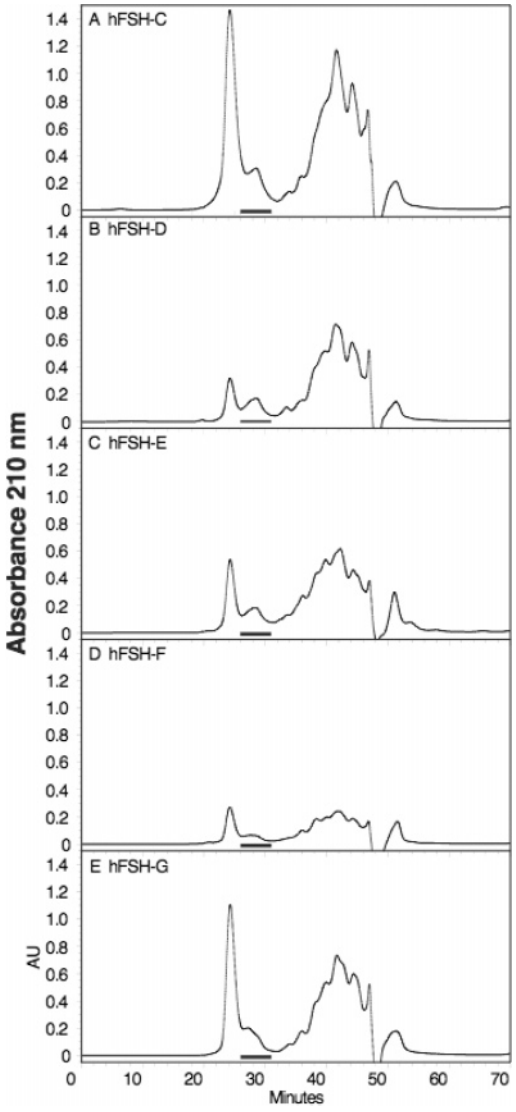

FIGURE 5: FSH isoform glycopeptide isolation. The Superdex peptide column was equilibrated with 0.2 M ammonium bicarbonate. The chromatograms were developed with the same mobile phase at a flow rate of 0.4 mL/min. Portions of the chromatograms pooled to obtain the glycopeptide fractions are indicated with the solid bars. (A) Glycopeptides derived from 795 μg of hFSH-C. (B) Glycopeptides derived from 252 μg of hFSH-D. (C) Glycopeptides derived from 380 μg of hFSH-E. (D) Glycopeptides derived from 127 μg of hFSH-F. (E) Glycopeptides derived from 670 μg of hFSH-G.

Table 5: Yield of ═PhNCS Amino Acid Derivatives at Each Edman Cycle for the Four Most Abundant hFSH-C Glycopeptides Adsorbed to Immobilon-P^{SQ} PVDF Membranes

site	cycle 1	cycle 2	cycle 3	cycle 4
αAsn^{52}	Lys	(Asn^{CHO})	Val	Thr
yield (pmol)	18.1	−	2.5	(4.6)
αAsn^{78}	(Asn^{CHO})	His	Thr	
yield (pmol)	−	6.3	(5.5)	
βAsn^{7}	(Asn^{CHO})	Ile	Thr	
yield (pmol)	−	2.8	(5.5)	
βAsn^{24}	Ile	(Asn^{CHO})	Thr	Thr
yield (pmol)	15.6	−	(5.5)	(4.6)

of the associated KNVT glycopeptide, as the cycle 3 yield of ═PhNCS-Val was substantially increased over that observed for the adsorbed peptide (Table 5). The yield of ═PhNCS-His was only modestly increased. However, this residue persisted at cycles 3 and 4, as if larger peptides, such

Table 6: Yield of ═PhNCS Amino Acid Derivatives at Each Edman Cycle for the Most Abundant hFSH-C Glycopeptides Covalently Attached to Sequelon-AA Arylamine-Derivatized PVDF Membranes

site	cycle 1	cycle 2	cycle 3	cycle 4
αAsn^{52}	Lys	(Asn^{CHO})[a]	Val	Thr
yield (pmol)	18.0	−	13.3	(16.9)[b]
αAsn^{78}	(Asn^{CHO})	His	Thr	
yield (pmol)	−	8.8	(21.4)	
βAsn^{7}	(Asn^{CHO})	Ile	Thr	
yield (pmol)	−	5.6	(21.4)	
βAsn^{24}	Ile	(Asn^{CHO})	Thr	Thr
yield (pmol)	15.7	−	(21.4)	(16.9)

[a] No ═PhNCS-Asn derivative was detected because glycosylated amino acid derivatives are extracted from the Edman cartridge. [b] Parentheses indicate combined yields from the same residue in different peptides.

as ENHT or VNHT, were present in the mixture. Indeed, reevaluation of Edman cycle 1 revealed both ═PhNCS-Val and ═PhNCS-Glu (not shown), while mass spectrometry analysis of hFSH-D glycopeptides identified two possessing the peptide ENHT (Table 7). Combining the yields of ═PhNCS-His for cycles 2−4 totaled 15.9 pmol, almost as much as the 18.0 pmol of ═PhNCS-Lys in cycle 1, thereby rationalizing the apparent low yield of αAsn^{78} glycopeptides based on recovery of cycle 2 ═PhNCS-His alone. The yield of ═PhNCS-Ile in cycle 2 remained low, consistent with partial glycosylation at this site. Similar results were obtained for all other hFSH isoform glycopeptide preparations described in this study as well as 15 other hFSH glycopeptide preparations derived from other hFSH preparations. Moreover, glycopeptides isolated from proteinase K digestion of a sample of hFSHα also resulted in greater yields of cycle 1 ═PhNCS-Lys than of cycle 2 ═PhNCS-His. Thus, despite the nonspecific nature of proteinase K, we consistently recovered the same glycopeptide populations from different hFSH isolates.

High-pH anion exchange chromatography was used to separate 2 nmol samples of the glycopeptide mixtures to assess the populations of glycans isolated from each isoform preparation. Samples of hFSH AFP-4161B glycopeptides were compared with the same-sized samples obtained from hFSH isoform preparations hFSH-C−hFSH-G (Figure 6).

Table 7: Mass Spectrometry Results

calcd mass	peptide	peak no.[a]	charge	hFSH AFP-4161B	hFSH-C	hFSH-D	hFSH-E	hFSH-F	hFSH-G
αAsn52									
1761.1647	KNVT	1	−2	1761.1703		1761.1565		1761.1818	1761.2052
1772.1559	KNVT	2	−2						1772.1679
1659.6250	KNVT	3	−2	1659.6407		1659.6291		1659.6364	1659.6542
1670.6162	KNVT	4	−2						1670.6169
1615.6170	KNVT	5	−2	1615.6196		1615.6194	1615.6153	1615.6364	
1626.6170	KNVT	6	−2						1626.6162
1514.0773	KNVT	7	−2		1514.0770	1514.0792	1514.0869	1514.1818	1514.0678
1525.0685	KNVT	8	−2		1525.0685				1525.0704
1534.5906	KNVT	9	−2		1534.5979	1534.5943		1534.6364	
1433.0509	KNVT	10	−2	1433.0389	1433.0509	1433.0516	1433.0563	1433.1818	1433.0425
1444.0421	KNVT	11	−2		1444.0421				1444.0406
1331.5112	KNVT	12	−2	1331.5149	1331.5112	1331.5114	1331.5161	1331.6364	1331.5179
1342.5024	KNVT	13	−2		1342.4984	1342.5050			1342.5049
1368.5296	KNVT	14	−2		1368.5397	1368.5280			
1206.4768	KNVT	15	−2			1206.4777			
1246.4552	KNVT	16	−2		1246.4559	1246.4554			1246.4592
1185.9635	KNVT	17	−2		1185.9732	1185.9642			
1267.4637	NVT	18	−2			1267.4655			
αAsn78									
1599.5857	EHNT					1599.5913			
1100.9114	ENHT					1100.9089			
βAsn24									
1726.1381	INTT	19	−2	1726.1460		1726.1395		1726.0909	1726.1457
1737.1294	INTT	20	−2						1737.1296
1682.1301	INTT	21	−2	1682.1180		1682.1349		1682.1818	1682.1134
1693.1214	INTT	22	−2			1693.1257			1693.1149
1580.5904	INTT	23	−2	1580.5947	1580.5904	1580.5931	1580.5909	1580.6364	1580.5999
1591.5817	INTT	24	−2		1591.5851	1591.5846	1591.5919	1591.6364	1591.5839
1499.5640	INTT	25	−2	1499.5776	1499.5640	1499.5662	1499.5632	1499.6364	1499.5718
1510.5553	INTT	26	−2		1510.5553	1510.5585			
1398.0243	INTT	27	−2	1398.0274	1398.0243	1398.0251	1510.5647	1398.0909	1510.5573
1409.0156	INTT	28	−2		1409.0156	1409.0164	1398.0319	1409.0909	1398.0276
1354.0163	INTT	29	−2	1354.0183	1354.0148	1354.0174	1409.0247	1354.0909	1409.0155
1312.9683	INTT	30	−2				1354.0091		1353.9956
1272.9899	INTT	31	−2			1272.9895	1312.9675		
1252.4766	INTT	32	−2	1252.4715	1252.4759	1252.4766	1252.4859	1252.6364	1252.4754
1069.9105	INTT	33	−2			1069.9107			1069.9142
1171.4502	INTT	34	−2		1171.4452	1171.4511			1171.4454
βAsn7									
1858.1804	NIT	35	−2			1858.1835			1858.2126
1347.5005	NIT	36	−2			1347.503			
1675.6143	NIT	37	−2			1675.6253			
1777.1540	NIT	38	−2			1777.1551			

[a] Refers to glycopeptide ions described in an earlier study describing FSH glycans (*15*).

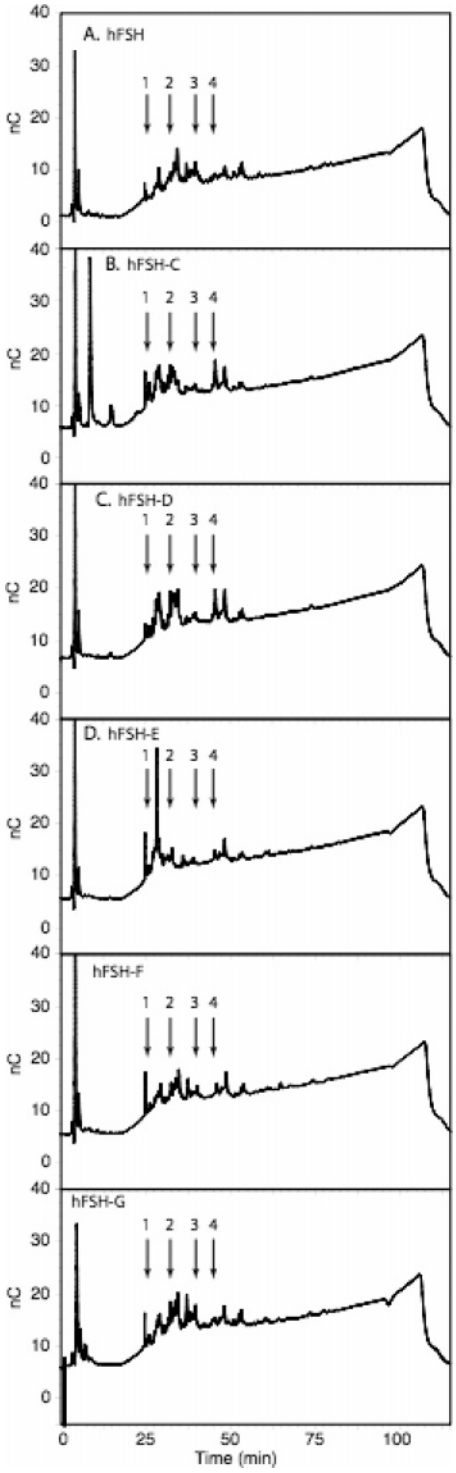

FIGURE 6: Glycopeptide fractionation. Samples (2 nmol) of glycopeptide preparations isolated in Figure 5 were fractionated by high-pH anion exchange chromatography and the glycan moieties detected by integrated pulsed amperometry using a Dionex carbohydrate analyzer. The column was a 4 mm × 250 mm CarboPac PA-100 column equilibrated with 100 mM sodium hydroxide at a flow rate of 0.5 mL/min. The chromatogram was developed with a 0 to 0.8 M sodium acetate gradient from 10 to 100 min. The arrows indicate the positions of one-, two-, three-, and four-branch glycans released from free hCGα Asn^{52} by PNGase digestion (*24*).

The bulk of the glycopeptides emerged between 25 and 60 min. Arrows indicate the elution times for hCGα oligosaccharides possessing one, two, three, or four sialic acid-terminated branches under the same chromatographic conditions (*24*). As the chromatography is affected by monosaccharide composition and linkage as well as negative charge, these emerge as clusters of peaks, particularly the three- and four-branch glycans. Each arrow indicates the position of the most abundant peak in each glycan cluster. The later elution times for some of the glycopeptide peaks do not necessarily imply the existence of five-branch glycans, because the reference hCGα glycans lacked the peptide components that also affect retention times. No enrichment of glycans with fewer branches in the less acidic isoforms was obvious, nor was there appreciable enrichment for glycans with more branches in the more acidic fractions. Only one isoform preparation stood out. The glycopeptide map for hFSH-E possessed a large peak emerging at 28 min, not found in other isoform glycopeptide preparations. This peak was in the region where neutral and single-branch glycans were typically eluted, which seemed at odds for the relatively low pI of 4.53.

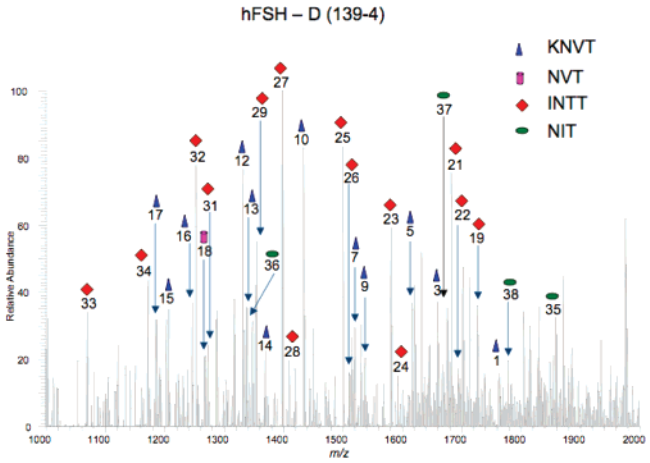

FIGURE 7: Glycopeptide analysis by mass spectrometry. Glycopeptides from three N-glycosylation sites in the hFSH isoform, hFSH-D, are identified in the spectrum, as indicated.

Glycopeptide mass spectrometry (Figure 7) identified both KNVT and INTT glycopeptides in every glycoform preparation (Table 7). Analysis of a 277 μg sample of AFP-4161B identified 12 of the 38 glycans identified in an earlier analysis of a 2 mg sample of the same preparation (*15*). Glycopeptides representing all four glycosylation sites were only identified in the hFSH-D glycopeptide mass spectrum. The glycopeptide ENHT was decorated with neutral glycans, which were probably tetra-antennary. It was interesting to note that the four-branch glycans were restricted to one site in each subunit: Asn^{78} in the α subunit and Asn^{7} in hFSHβ.

FSH isoform gel filtration revealed three major fractions associated with each FSH preparation (Figure 8). Aggregated hFSH emerged first as a series of three overlapping peaks, followed next by a large heterodimer peak, and finally by a FSH subunit peak. The aggregated hFSH fraction consisted of four high-MW bands according to hFSHβ-specific Western blot analysis of hFSH AFP-4161B and hFSH-G (Figure 8F, inset). The heterodimer peak was composed primarily of the hFSH band, although aggregated hFSH and subunit bands from these partially overlapping peaks could also be discerned. Western blotting of the subunit peak revealed that its major component migrated in the subunit region of the gel, although some immunoactivity migrated in the heterodimer region as well. The latter was presumably derived from the partially overlapping heterodimer peak. Most of

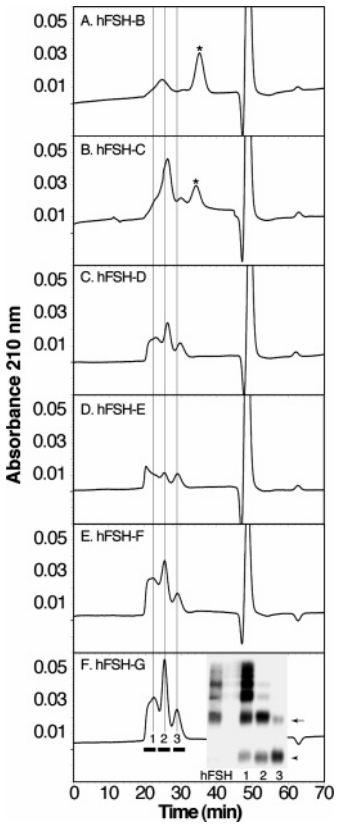

FIGURE 8: Comparison of hFSH isoform preparations by Superdex 75 gel filtration. Samples (10 μg) of each isoform preparation were subjected to gel filtration as described in Experimental Procedures. Lines indicating the retention times for the three peaks in panel G are provided to facilitate comparison of the three fractions (1, aggregated hFSH; 2, hFSH heterodimer; 3, hFSH subunits). The asterisks in panels A and B indicate residual ampholine peaks: (A) hFSH-B, (B) hFSH-C, (C) hFSH-D, (D) hFSH-E, (E) hFSH-F, and (F) hFSH-G. The inset of panel F shows the FSHβ-specific Western blot of portions of the chromatogram indicated by solid bars. SDS−PAGE of aggregated hFSH (1), the putative hFSH heterodimer (2), and hFSH subunits (3), as indicated, was carried out under nonreducing conditions. The primary antibody was anti-FSHβ monoclonal antibody RFSH20. A sample of hFSH (AFP-4161B) was included for comparison. The arrow indicates the position of the hFSH heterodimer band, and the arrowhead indicates the position of the β subunit band.

the less active hFSH isoform preparation heterodimers emerged in a symmetric peak. The hFSH-C isoform heterodimer peak appeared to consist of two partially resolved components. The later-emerging, smaller-sized component appeared to be more abundant, and the conformation resulting in the smaller apparent molecular size is potentially significant because this preparation exhibited the highest FSH receptor binding activity. Also notable was the relative absence of high-MW aggregated hFSH species in hFSH-C.

DISCUSSION

Chromatofocusing has been used extensively to characterize changes in FSH isoform abundance associated with different physiological states (*7*). The underlying assumption is that hFSH isoforms are separated on the basis of differences in negative charge due to variability in terminal sialic acid content or, to a much lesser extent in hFSH, terminal sulfate content (*12*−*15*). Charge heterogeneity is only partially related to glycan structure as incomplete sialylation and sulfation both occur in FSH such that glycan branch number does not always correspond to the number of negative charges (*13*−*15*). The all-or-none glycosylation of hFSHβ provides a second mechanism for varying the overall net charge by providing one glycoform population possessing only two N-glycans and another possessing all four N-glycans (*11*). Heterogeneous glycan branching in similarly charged FSH isoforms was suggested as an obvious consequence of selection on the basis of overall charge that could be overcome by subsequent anion exchange chromatography because the latter selects on the basis of surface charge (*25*). While a series of hFSH isoforms possessing 1.3−13 sialic residues per molecule were isolated using this combination of techniques (*9*), electrophoretic patterns following SDS−PAGE showed two partially overlapping Coomassie blue-stained bands which suggested both di- and tetraglycosylated hFSH glycoforms were present in each isoform fraction (*8*). Chromatofocusing followed by lectin affinity chromatography revealed underlying glycan structural heterogeneity associated with assumed common overall charge (*26*).

In this study, both major hFSH glycoforms were present in most hFSH isoform preparations separated by chromatofocusing. Moreover, these hFSH isoforms were not even enriched for glycans possessing the same number of terminal, charged sialic acid residues or sulfate moieties. Western blot analysis revealed no pattern of di- and tetraglycosylated hFSH glycoform abundance that could be related to the numbers of glycans attached, such as high-pI isoforms either enriched for or exclusively diglycosylated hFSH, intermediate-pI isoforms possessing both glycoforms, and low-pI isoforms such as enriched or exclusively tetraglycosylated hFSH. For example, hFSH-B, the least acidic isoform preparation, did not possess exclusively diglycosylated hFSH, which was observed in our previous study (*11*). Instead, it consisted of tetraglycosylated hFSH and a novel variant with an even more retarded hFSHβ subunit band mobility that implied large glycan size despite the high pI associated with the fraction. The absence of an exclusively diglycosylated hFSH fraction could be rationalized by more complete removal of hLH from the AFP-4161B preparation by A. F. Parlow. The hFSH isoform preparation possessing exclusively diglycosylated hFSH in our earlier study included the highest level of hLH contamination, which had to be removed by immunoaffinity chromatography (*11*). Less acidic hFSH isoform fractions prepared by other investigators are also known to possess hLH contamination (*27*). At the other end of the chromatogram, while the most acidic isoform preparation, hFSH-G, possessed 70% tetraglycosylated hFSH, hFSH-E was almost exclusively composed of this glycoform, despite being less acidic.

Glycopeptide mass spectrometry provided strong evidence that chromatofocusing failed to separate hFSH isoforms on the basis of N-glycan structure or charge. This analysis, which characterizes complete glycan structures, including terminal charged residues, revealed a range of negatively charged glycans in all hFSH isoform preparations. While the less acidic hFSH isoform preparation hFSH-C was decorated with both αAsn^{52} and βAsn^{24} glycans bearing one or two negative charges, hFSH-D glycans possessed one to three negatively charged residues at both sites. The most acidic isoform preparation, hFSH-G, possessed two or three negative charges in the αAsn^{52} glycans and one to three negative

charges in the βAsn^{24} glycans. Considerable glycan structure overlap was observed when the most active and least active isoform preparations were compared.

The hFSH isoform preparations examined in this study exhibited classic isoform behavior in radioimmunoassays and radioligand receptor assays. Two radioimmunoassays detected an up to 2-fold range of FSH immunoactivities in all but one hFSH isoform preparation, while two FSH receptor binding assays indicated greater than 10- or 20-fold ranges of FSH receptor binding activities (the actual range could not be determined because not all isoform preparations displaced 50% of the tracer). The total hFSH immunoactivity recovery from chromatofocusing fractionation ranged from 65 to 87%, while biological activity recovery was only 5% in the rat testis FSH RLA and 3% when human receptors were employed. Part of the low activity in the FSH receptor binding assay was related to the nature of the [^{125}I]eFSH tracer. We use this tracer because iodination at eFSHα Tyr residue 21, 87, or 93 is more compatible with FSHR binding (specific binding of 25−35% of the total counts per minute added) than iodination at hFSHα Tyr residues 88 and 89 (1.5% of the total counts per minute added), which are both buried in the FSH−FSHR interface (*28*). Horse FSH also possesses partially (βAsn^{24} glycosylated) and fully glycosylated FSHβ subunit variants (*29*). Approximately 90% eFSH possesses the partially glycosylated β subunit. Recent studies with isolated di- and tetraglycosylated hFSH preparations revealed a 26-fold greater receptor binding activity for diglycosylated hFSH as compared to tetraglycosylated hFSH in the rat testis FSH receptor assay. The eFSH included in these studies exhibited slightly higher binding activity than diglycosylated hFSH, making it functionally equivalent to the more active human glycoform. The activity of 75% tetraglycosylated hFSH AFP-4161B was very similar to that of purified tetraglycosylated hFSH (G. R. Bousfield and V. Y. Butnev, unpublished observations). Isoform hFSH-E, which exhibited no detectable FSH receptor binding activity, possessed 81% immunological activity relative to the purified hFSH preparation AFP-4161B, from which it was derived, in the RFSH20 (hFSHβ-specific) RIA. The amount of hFSH immunological activity was significantly greater than that associated with the most active isoform preparation in the RLA, hFSH-C (59%), most likely because of the lower subunit content of the latter preparation. The relative activities of hFSH-C (72%) and hFSH-E (59%) were reversed in the α epitope-directed FSH25 radioimmunoassay, which measured hFSH heterodimer, consistent with the greater heterodimer content of hFSH-C. Even so, hFSH-C was only 22% more active than hFSH-E. Despite their similar immunological activities in two separate radioimmunoassays, hFSH-C was 47−74% as active as AFP-4161B in both human and rat FSH radioligand receptor assays, while hFSH-E exhibited no detectable receptor binding activity in either assay. However, the receptor binding differences could not be rationalized by the presence or absence of specific glycans because of considerable overlap in the glycan populations present in each isoform preparation. At αAsn^{52}, the most important site for hFSH function (*30*, *31*), three of four αAsn^{52} glycans present in the hFSH-E glycan population were also present in the 10-glycan hFSH-C glycopeptide population. At βAsn^{24}, seven of nine hFSH-E glycans had counterparts in the nine-glycan hFSH-C βAsn^{24} glycopeptide population. As no αAsn^{78} or βAsn^{7} glycans were detected in most isoform preparations, we could compare glycosylation of hFSH-C and hFSH-E at only the other two sites.

In our earlier study of a larger hFSH glycopeptide preparation also derived from AFP-4161B, we detected glycopeptide ions associated with three of four hFSH glycosylation sites. In that study, 26% of the glycopeptides were eluted earlier in the chromatogram prior to the main glycopeptide peak. Nevertheless, Edman degradation indicated that the glycopeptide fraction characterized by mass spectrometry possessed glycans from all four N-glycosylation sites (*15*). Elimination of the protease peak by graphitized charcoal adsorption also eliminated the glycopeptides associated with higher-molecular weight fractions. As four-branch glycans appeared to be restricted to αAsn^{78} and βAsn^{7}, the under-represented glycopeptides, other large glycans attached to both sites might not have been present in the isoform glycopeptide fractions that we analyzed. However, this is unlikely, as smaller βAsn^{7} glycans were detected in the earlier study employing a larger hFSH sample. Moreover, Edman degradation indicated both αAsn^{78} and βAsn^{7} glycopeptides were present in the glycopeptide fractions employed in this study. The apparent low yield of αAsn^{78} glycopeptides appeared to be related to the existence of four- and five-residue peptides incorporating the Asn-His-Thr peptide, which was confirmed by detection of the ENHT tetrapeptide in the hFSH-D glycopeptide mass spectrum. Time-related loss of glycopeptide signals in mass spectrometry experiments was noted in the earlier study. This is the first time Edman degradation also showed site-specific loss of a glycopeptide population that corresponded to the missing glycopeptide ions. However, as glycopeptide preparations could be analyzed by high-pH anion exchange chromatography even after the loss of all glycopeptide signals in mass spectrometry experiments, application of the analytical chromatographic procedure to hFSH isoform glycopeptide analysis provided additional evidence of the failure of chromatofocusing to separate hFSH isoforms on the basis of differences in glycan structure.

Glycopeptide mapping confirmed extensive similarities with some differences in glycan populations derived from different hFSH isoform preparations. While the individual components of each peak could not be identified due to the low abundance of glycopeptide and high salt concentration of the HPLC mobile phase, peak heights have been shown to indicate glycan abundance when oligosaccharides are separated by this method (*3*). Neutral glycans, known to comprise 5−10% of hFSH oligosaccharides (*13*, *14*), were eluted between 16 and 27 min, while sialylated oligosaccharides with one to four branches were eluted between 25.5 and 45 min. Biantennary glycans terminated with one sulfate and one sialic acid were eluted at 48 min. As high-pH anion exchange chromatography separation involves several glycan structural features, including branch number, composition, fucosylation, bisecting GlcNAc residues, and linkage, as well as negative charge (*32*), most hFSH glycopeptides should emerge in groups clustered near the positions indicated by the arrows in Figure 6. The expected trend of enrichment for clusters of smaller and neutral glycopeptide peaks in the less acidic fractions and clusters of larger glycopeptide peaks in the more acidic fractions, as suggested by glycopeptide gel filtration, was not supported by the widespread distribu-

tion of glycopeptide peaks in the glycan mapping chromatograms. Taken together, both mass spectrometry and high-pH anion exchange chromatography data were consistent with the absence of enrichment for smaller glycans bearing fewer negative charges in the less acidic isoforms and larger, more negatively charged glycans in the more acidic isoform preparations. Despite the considerable overlap in glycosylation, significant functional differences were observed for the isoform preparations.

FSH aggregation as indicated in the Western blots and gel filtration analysis was an attractive mechanism for rationalizing both the failure of chromatofocusing to separate hFSH on the basis of glycosylation and the near total absence of biological activity in most isoform preparations. Gel filtration and nonreducing SDS−PAGE suggested the existence of at least three aggregated hFSH forms in addition to the heterodimer in each isoform preparation. These could have provided numerous combinations of glycan populations with the same overall net charge that resulted in the apparent absence of glycan separation by chromatofocusing. Aggregation with other proteins might also provide an explanation for the effects of different sources and degrees of purity on hFSH isoform patterns (*7*). The loss of receptor binding activity and retention of immunological activity might be explained by the different locations of the receptor binding site and antibody epitopes. Two subunit-specific antibodies that recognized opposite ends of the FSH molecule bound aggregated hFSH: monoclonal antibody HT13, which recognized α subunit residues 15−17 in loop αL1 and residues 72−75 in loop αL3 (*33*), and RFSH20, which recognized FSHβ residues 67−72, located in loop βL3 (*34*). The receptor binding surface is located on one side of the FSH molecule and consists of cystine knot loop 2 in each subunit, as well as the hFSHβ seatbelt loop (*28*). Side-by-side aggregation of hFSH molecules would render the receptor binding site inaccessible, yet the antibody epitopes on both ends of hFSH would remain accessible. The gel filtration data were particularly important indicators of FSH aggregation in solution, as we know from experience with oLH that aggregation can appear following SDS−PAGE for samples isolated from the heterodimer fraction of a gel filtration column, particularly under nonreducing conditions (*35*). However, no aggregation was apparent during removal of ampholine by Sephadex G-75 gel filtration, which immediately followed chromatofocusing. The delayed appearance of aggregated hFSH suggested aggregation was a storage phenomenon, because these isoform preparations were isolated several years ago and because hFSH preparations are known to deteriorate over time. However, AFP-4161B, the hFSH preparation from which the isoform preparations were derived, was stored under identical conditions for the same length of time yet was comprised of only 20% aggregated forms and 8% subunit, as assessed by gel filtration. The 72% heterodimer content was greater than that of the low-activity hFSH isoform preparation heterodimer fraction, which ranged from 25 to 43%. Although these values were lower than that for AFP-4161B, if the putative heterodimer peak relative abundance was an indication of FSH bioactivity, all of these isoform preparations would have produced complete inhibition curves in the radioligand assay. For example, the biological activities for hFSH-C and hFSH-E differed by at least 23-fold, while their heterodimer peak areas differed by only 6-fold. This implies that the majority of hFSH-E heterodimer is nonfunctional, possibly due to conformational change, which is difficult to demonstrate. Inactive LH heterodimers generally result from interspecific combinations of complementary subunits, such as hCGα, oLHα, or pLHα combined with eLHβ (*36*). Because gel filtration has been recommended as a method for assessing purified hFSH preparations (*25*, *37*), the existence of nonfunctional heterodimers suggests a potentially serious flaw in this approach.

Gel filtration of hFSH isoform samples provided evidence of a physical difference between the most active isoform preparation, hFSH-C, which was eluted as an asymmetric peak encompassing two overlapping components, and the other less active isoform preparations. Most of the absorbance was associated with the smaller hFSH-C heterodimer peak component, which had a retention time of 26.2 min. The aggregated material, encountered in the other low-activity isoform fractions as two or three overlapping peaks, was reduced to a leading shoulder. All other more acidic hFSH isoform preparation heterodimer fractions were eluted as a symmetrical peak, preceded by overlapping aggregated hFSH peaks. The chromatogram for isoform hFSH-E, which lacked detectable FSH receptor binding activity, indicated a retention time of 25.6 min for the hFSH peak. This earlier retention time matched the leading shoulder component of the hFSH-C putative heterodimer fraction. The structural feature responsible for the later elution of the major component of hFSH-C remains unknown but is unlikely to be glycosylation, given the degree of overlap between hFSH-C glycan populations and those of isoforms hFSH-D−hFSH-G.

Chromatofocusing has been used extensively to characterize changes in FSH associated with different physiological states (*7*). A critical issue emerging from our studies is how generally our observation of variations in hFSH isoform receptor binding activity despite similar glycoform abundance and glycan populations can be applied to hFSH isoforms described in other studies. One difference between our studies and most other studies is the fact that we have fractionated purified hFSH preparations instead of crude tissue extracts or physiological fluids containing low concentrations of hFSH along with many other proteins. The only other series of studies involving purified hFSH isoforms employed isoelectric focusing as the initial phase of the fractionation procedure (*8*−*10*). The outcome of that series of investigations was unique in that the more acidic isoforms exhibited greater FSH receptor binding activity than the less acidic isoforms (*8*). In fact, there was a significant correlation between high receptor binding activity and high sialic acid content (*10*). However, the broad Coomassie-stained bands following SDS−PAGE of those hFSH preparations suggested the presence of both diglycosylated and tetraglycosylated hFSH glycoforms in hFSH isoform preparations obtained by isoelectric focusing. FSH isoform patterns for crude samples, such as pituitary extracts, serum, and urinary derivatives, were strikingly different, suggesting differential FSH secretion by the pituitary and extensive FSH metabolism in the kidney or selective retention of FSH isoforms by other organs, such as the liver (*7*). However, chromatofocusing of commercially produced postmenopausal urinary gonadotropin preparations of varying purity also resulted in striking alterations in FSH isoform populations, which suggested that

the FSH isoform patterns were influenced by the presence or absence of other proteins. For the gonadotropin isoform field to move forward, separation methods of separating gonadotropin preparations on the basis of differences in glycosylation and maintaining the functional integrity of the hormone will have to be developed.

CONCLUSION

Chromatofocusing separated purified hFSH into seven isoform fractions, which exhibited similar immunological activities and widely varying receptor binding activities. Mass spectrometry and high-pH anion exchange chromatography indicated a high degree of overlap in glycan populations associated with each hFSH isoform preparation, indicating that chromatofocusing did not separate these on the basis of glycan structure. Evidence of aggregation was obtained following SDS−PAGE under reducing conditions and gel filtration under native conditions. However, because gel filtration indicated there was sufficient heterodimer fraction in each preparation to displace receptor assay tracer, the mechanism that accounts for the significant divergence between FSH immunological activity and FSH biological activity remains unknown.

ACKNOWLEDGMENT

We acknowledge the highly purified hFSH provided by the National Hormone and Pituitary Program and Dr. A. F. Parlow. The hFSH isoform preparations employed in this study were purified by Dr. Hiromu Sugino in Dr. Darrell N. Ward's laboratory at M. D. Anderson Cancer Center.

REFERENCES

1. Bousfield, G. R., Jia, L., and Ward, D. N. (2006) Gonadotropins: Chemistry and biosynthesis, in *Knobil and Neill: Physiology of Reproduction* (Neill, J. D., Ed.) pp 1581−1634, Elsevier, San Diego.
2. Hearn, M. T. W., and Gomme, P. T. (2000) Molecular architecture and biorecognition processes of the cystine knot protein superfamily: Part I. The glycoprotein hormones, *J. Mol. Recognit. 13*, 223−278.
3. Bousfield, G. R., Butnev, V. Y., Butnev, V. Y., Nguyen, V. T., Gray, C. M., Dias, J. A., MacColl, R., Eisele, L., and Harvey, D. J. (2004) Differential effects of α asparagine^{56} oligosaccharide structure on equine Lutropin and Follitropin hybrid conformation and receptor-binding activity, *Biochemistry 43*, 10817−10833.
4. Weisshaar, G., Hiyama, J., and Renwick, A. G. C. (1991) Site-specific N-glycosylation of human chorionic gonadotropin: Structural analysis of glycopeptides by one- and two-dimensional ^{1}H NMR spectroscopy, *Glycobiology 1*, 393−404.
5. Liu, C., and Bowers, L. D. (1997) Mass spectrometric characterization of nicked fragments of the β-subunit of human chorionic gonadotropin, *Clin. Chem. 43*, 1172−1181.
6. Valmu, L., Alfthan, H., Hotakainen, K., Birken, S., and Stenman, U. H. (2006) Site-specific glycan analysis of human chorionic gonadotropin β-subunit from malignancies and pregnancy by liquid chromatography−electrospray mass spectrometry, *Glycobiology 16*, 1207−1218.
7. Ulloa-Aguirre, A., Midgley, A. R., Jr., Beitins, I. Z., and Padmanbhan, V. (1995) Follicle-stimulating isohormones: Characterization and physiological relevance, *Endocr. Rev. 16*, 765−787.
8. Stanton, P. G., Robertson, D. M., Burgon, P. G., Schmauk-White, B., and Hearn, M. T. W. (1992) Isolation and physicochemical characterization of human follicle-stimulating hormone isoforms, *Endocrinology 130*, 2820−2832.
9. Stanton, P. G., Shen, Z., Kecorius, E. A., Bergon, P. G., Roberson, D. M., and Hearn, M. T. (1995) Application of a sensitive HPLC-based fluorometric assay to determine the sialic acid content of human gonadotropin isoforms, *J. Biochem. Biophys. Methods 30*, 37−48.
10. Stanton, P. G., Burgon, P. G., Hearn, M. T. W., and Robertson, D. M. (1996) Structural and functional characterization of hFSH and hLH isoforms, *Mol. Cell. Endocrinol. 125*, 133−141.
11. Walton, W. J., Nguyen, V. T., Butnev, V. Y., Singh, V., Moore, W. T., and Bousfield, G. R. (2001) Characterization of human follicle-stimulating hormone isoforms reveals a non-glycosylated β-subunit in addition to the conventional glycosylated β-subunit, *J. Clin. Endorinol. Metab. 86*, 3675−3685.
12. Green, E. D., and Baenziger, J. U. (1988) Asparagine-linked oligosaccharides on lutropin, follitropin, and thyrotropin: I. Structural elucidation of the sulfated and sialylated oligosaccharides on bovine, ovine and human pituitary glycoprotein hormones, *J. Biol. Chem. 263*, 25−35.
13. Green, E. D., and Baenziger, J. U. (1988) Asparagine-linked oligosaccharides on lutropin, follitropin, and thyrotropin II. distributions of sulfated and sialylated oligosaccharides on bovine, ovine, and human pituitary glycoprotein hormones, *J. Biol. Chem. 263*, 36−44.
14. Renwick, A. G. C., Mizuochi, T., Kochibe, N., and Kobata, A. (1987) The asparagine-linked sugar chains of human follicle-stimulating hormone, *J. Biochem. 101*, 1209−1221.
15. Dalpathado, D. S., Irungu, J. A., Go, E. P., Butnev, V. Y., Norton, K., Bousfield, G. R., and Desaire, H. (2006) Comparative glycomics of the glycoprotein hormone follicle-stimulating hormone (FSH): Glycopeptide analysis of isolates from two mammalian species, *Biochemistry 45*, 8665−8673.
16. Jiang, H., Butnev, V. Y., Bousfield, G. R., and Desaire, H. (2004) Glycoprotein profiling by electrospray mass spectrometry, *J. Am. Soc. Mass Spectrom. 15*, 750−758.
17. Irungu, J. A., Dalpathado, D. S., Go, E. P., Jiang, H., Ha, H.-V., Bousfield, G. R., and Desaire, H. (2006) A Method for Characterizing Sulfated Glycoproteins in a Glycosylation Site-Specific Fashion, Using Ion-Pairing and Tandem Mass Spectrometry, *Anal. Chem. 78*, 1181−1190.
18. Calvo, F. O., Keutmann, H. T., Bergert, E. R., and Ryan, R. J. (1986) Deglycosylated human follitropin: Characterization and effects on adenosine cyclic 3′,5′-phosphate production in porcine granulosa cells, *Biochemistry 25*, 3938−3943.
19. Gordon, W. L., Bousfield, G. R., and Ward, D. N. (1989) Comparative binding of FSH to chicken and rat testis, *J. Endocrinol. Invest. 12*, 383−392.
20. Bidart, J.-M., Troalen, F., Lazar, V., Berger, P., Marcillac, I., Lhomme, C., Droz, J.-P., and Bellet, D. (1992) Monoclonal antibodies to the free β-subunit of human chorionic gonadotropin define three distinct antigenic domains and distinguish between intact and nicked molecules, *Endocrinology 131*, 1832−1840.
21. Butnev, V. Y., Gotschall, R. R., Baker, V. L., Moore, W. T., and Bousfield, G. R. (1998) Hormone-specific inhibitory influence of α-subunit Asn^{56} oligosaccharide on *in vitro* subunit association and FSH receptor binding of equine gonadotropins, *Biol. Reprod. 58*, 458−469.
22. Gotschall, R. R., and Bousfield, G. R. (1996) Oligosaccharide mapping reveals hormone-specific glycosylation patterns on equine gonadotropin α-subunit Asn^{56}, *Endocrinology 137*, 2543−2557.
23. Bousfield, G. R., Butnev, V. Y., Walton, W. J., Nguyen, V. T., Singh, V., Hueneidi, J., Kolli, K., Harvey, D. J., and Rance, N. (2007) All or none N-glycosylation in primate follicle-stimulating hormone subunits, *Mol. Cell. Endocrinol. 260−262*, 40−48.
24. Bousfield, G. R., Baker, V. L., Gotschall, R. R., Butnev, V. Y., and Butnev, V. Y. (2000) Carbohydrate analysis of glycoprotein hormones, *Methods 21*, 15−39.
25. Johnston, R. C., Stanton, P. G., Robertson, D. M., and Hearn, M. T. (1987) High-performance liquid chromatography of amino acids, peptides and proteins. LXXXV. Separation of isoforms of the glycoprotein hormones from human pituitary extracts, *J. Chromatogr. 397*, 389−398.
26. Creus, S., Chaia, Z., Pellizzari, E. H., Cigorraga, S. B., Ulloa-Aguirre, A., and Campo, S. (2001) Human FSH isoforms: Carbohydrate complexity as determinant of in-vitro bioactivity, *Mol. Cell. Endocrinol. 174*, 41−49.
27. Timossi, C. M., Barrios de Tomasi, J., Zambrano, E., Gonzalez, R., and Ulloa-Aguirre, A. (1998) A naturally occurring basically charge human follicle-stimulating hormone (FSH) variant inhibits FSH-induced androgen aromatization and tissue-type plasminogen activator enzyme activity in vitro, *Neuroendocrinology 67*, 153−163.

28. Fan, Q. R., and Hendrickson, W. A. (2005) Structure of human follicle-stimulating hormone in complex with its receptor, *Nature 433*, 269−277.
29. Bousfield, G. R., Butnev, V. Y., Gotschall, R. R., Baker, V. L., and Moore, W. T. (1996) Structural features of mammalian gonadotropins, *Mol. Cell. Endocrinol. 125*, 3−19.
30. Bishop, L. A., Robertson, D. M., Cahir, N., and Schofield, P. R. (1994) Specific roles for the asparagine-linked carbohydrate residues of recombinant human follicle stimulating hormone in receptor binding and signal transduction, *J. Mol. Endocrinol. 8*, 722−731.
31. Flack, M. R., Froehlich, J., Bennet, A. P., Anasti, J., and Nisula, B. C. (1994) Site-directed mutagenesis defines the individual roles of the glycosylation sites on follicle-stimulating hormone, *J. Biol. Chem. 269*, 14015−14020.
32. Townsend, R. R., and Hardy, M. R. (1991) Analysis of glycoprotein oligosaccharides using high-pH anion exchange chromatography, *Glycobiology 1*, 139−147.
33. Couture, L., Remy, J. J., Rabesona, H., Troalen, F., Pajot-Augy, E., Bozon, V., Haertle, T., Bidart, J. M., and Salesse, R. (1996) A defined epitope on the human choriogonadotropin α-subunit interacts with the second extracellular loop of the transmembrane domain of the lutropin/choriogonadotropin receptor, *Eur. J. Biochem. 241*, 627−632.
34. Robert, P. (1995) in *Pharmaceutical Sciences*, pp 101, Université René Descartes de Paris, Paris.
35. Bousfield, G. R., and Ward, D. N. (1994) Evidence for two folding domains in glycoprotein hormone α subunits, *Endocrinology 135*, 624−635.
36. Bousfield, G. R., Liu, W.-K., and Ward, D. N. (1985) Hybrids from equine LH: α enhances, *β* diminishes activity, *Mol. Cell. Endocrinol. 40*, 69−77.
37. Louriero, R. F., de Oliveira, J. E., Torjesen, P. A., Bartolini, P., and Ribela, M. T. C. P. (2006) Analysis of intact human follicle-stimulating hormone preparations by reversed-phase high-performance liquid chromatography, *J. Chromatogr., A 1136*, 10−18.

BI701764W